CALCULATION OF THE LONGITUDINAL ELASTIC ELECTRON SCATTERING FORM FACTORS FOR SOME LIGHT NUCLEI

حساب عوامل التشكل للاستطارة الالكترونية الطولية المرنة لبعض النوى الخفيفة

عادل خلف حمودي* و رعد عبدالكريم راضي* و فاضل إسماعيل شراد الطائي**

A. K. Hamoudi *, R. A. Radhi * and F.I. Shrrad Al-Taie **

*University of Baghdad-College of Science – Department of Physics

**University of Karbala-College of Science – Department of Physics

ABSTRACT:

The effects of the two-body short range correlation (SRC's) and the occupation probability (η) of higher states on the elastic electron scattering longitudinal form factors *F(q)*'s are investigated. Considering the effect of higher occupation probabilities and the effect of SRC's are important in getting good agreement between the calculated elastic longitudinal electron scattering *F(q)*'s and those of experimental data for ^{4}He, ^{12}C, ^{16}O, ^{28}Si, ^{32}S and ^{40}Ca nuclei.

الخلاصة :

درس تأثير كل من دالة ترابط الجسيمين القصير المدى (SRC) واحتمالية الأشغال للمستويات العليا (η) على عوامل التشكل للاستطارة الالكترونية الطولية المرنة *F(q)*'s. إن إدخال تأثير كل من احتمالية الأشغال (η) للمستويات العالية و دالة ترابط الجسيمين القصير المدى (SRC) في الحسابات له أهمية كبيرة في الحصول على توافق جيد بين النتائج العملية والنظرية لعوامل التشكل للاستطارة الالكترونية الطولية المرنة *F(q)*'s ولجميع النوى قيد الدراسة (^{4}He, ^{12}C, ^{16}O, ^{28}Si, ^{32}S and ^{40}Ca).

INTRODUCTION:

The scattering of electrons from nuclei give the most precise information about nuclear size and charge distribution, and it provides important information about the electromagnetic currents inside the nuclei. Electron scattering can provide a good test for such calculation since it is sensitive to the spatial dependence of the charge and current densities [1,2,3].

The electron – nucleus interaction is considered [4] in the first Bon approximation as an exchange of virtual photon carrying a momentum transfer q. In this case the initial and the final particles are considered free and can be represented by plan wave.

According to Born approximation the interaction of the electron with charge distribution of nucleus is considered as an exchange of a virtual photon with zero angular momentum along the direction of q, this is called longitudinal or Coulomb scattering.

The effect of the short range correlation due to the repulsive part of two-body interaction on the charge form factor of several p-shell nuclei has been analyzed in detail [5] with an independent particle model (IPM) generated in the harmonic oscillator (HO) well [6,7]. In ref [5], it was shown that the high-momentum parts ($q>3$ fm^{-1}) of the form factors calculated with and without correlations behave in completely different ways, which indicates that electron scattering at high momentum transfer could give useful information on the short-range correlations. The form factors measurement were reported by Bergstrom et.al. [8] for the electroexcitation of the 0^{+} (6.052-MeV), 3^{-} (6.131-MeV) and 2^{+} (6.916-MeV) states of ^{16}O, in the momentum transfer region 0.5 to 1.0 fm^{-1}. The data were compared with the predictions of various particle-hole shell models and a two-component phenomenological model.The elastic electron scattering cross section for the nucleus ^{12}C was measured in momentum transfer range of 0.25 to 2.75 fm^{-1}. The data were analyzed in a model independent way with Fourier-Bessel parameterization of the charge distribution. For the

root mean square (rms) radius, the value of $\langle r^2 \rangle^{1/2}$ =(2.464±0.012) fm was obtained. This value agrees with those of other electron scattering experiments and with muonic atom experiments but disagrees with the data obtained from measurements of muonic X-ray transitions with a crystal spectrometer which shows a larger rms radius, measured by Reuter et. al. [9]. Massen and Moustakidis [10,11] derived analytical expressions of the one and two body terms in the cluster expansion of the charge form factors and density distributions of sp- and sd- shell nuclei with Z=N. Those expressions were used for the systematic study of the effect of short range correlations on the form factors and densities, and they depend on the parameters *b* and *β*, which represent the harmonic oscillator parameter and the correlation parameter, respectively. These parameters were determined for various sp- and sd- shell nuclei by fitting the theoretical charge form factor to the experimental one. Electron scattering Coulomb form factors for the single-particle quadrupole transition in 1p and sd- shell nuclei have been studied by Radhi [12] taking into account the core-polarization effects, derived from the first-order perturbation theory. The inclusion of these effects modified the form factors markedly and described the experimental data very well.

THEORY

Elastic electron scattering form factor from spin zero nuclei **(** $J = 0$ **)**, can be determined by the ground – state charge density distributions (CDD). In the Plane Wave Born Approximation (PWBA), the incident and scattered electron waves are considered as plane waves and the CDD is real and spherical symmetric, therefore the form factor is simply the Fourier transform of the CDD. Thus: [13,14,15]

$$F(q) = \frac{4\pi}{Z} \int_0^\infty \rho_o(r)\, j_0(qr)\, r^2 dr \qquad (1)$$

where $\rho_o(r)$ is the ground state 2BCDD.

$j_0(qr) = Sin(qr)/(qr)$ is the zeroth order of the spherical Bessel function and q is the momentum transfer from the incident electron to the target nucleus. Eq. (1) can be expressed as

$$F(q) = \frac{4\pi}{qZ} \int_0^\infty \rho_o(r)\, Sin(qr)\, r\ dr \qquad (2)$$

Inclusion of the finite nucleon size correction $F_{fs}(q)$ and the center of mass correction $F_{cm}(q)$ in our calculations requires multiplying the form factor of eq (2) by these corrections. $F_{fs}(q)$ is considered as free nucleon form factor and assumed to be the same for protons and neutrons. This correction takes the form [16].

$$F_{fs}(q) = e^{-0.43q^2/4} \qquad (3)$$

and the correction $F_{cm}(q)$ removes the spurious state arising from the motion of the center of mass when shell model wave function is used and given by:

$$F_{cm}(q) = e^{q^2b^2/4A} \qquad (4)$$

where *A* is the nuclear mass number. Introducing these corrections into eq (2), we obtain

$$F(q) = \frac{4\pi}{qZ} \int_0^\infty \rho_o(r)\, Sin(qr)\, r\ dr\, F_{fs}(q)\, F_{cm}(q) \qquad (5)$$

In the limit of $q \to 0$, the target will be considered as a point particle, and from eq.(1) with the help of the following equation,

$$Z = 4\pi \int_0^\infty \rho_o(r)\ r^2\ dr \qquad (6)$$

the form factor of this target nucleus is equal to unity, i.e. $F(q \to 0)=1$. The elastic longitudinal electron scattering form factor with the inclusion of the effect of the short-range correlation in light nuclei can now be obtained by introducing the ground state 2BCDD of Ref.[15] together with those of eqs.(3) and (4) into eq (5). We also wish to mention that we have written all computer programs needed in this study by the languages of Fortran 90 power station .

RESULTS, DISCUSSION AND CONCLUSIONS

The elastic electron scattering longitudinal form factors *F(q)* from the considered spin-zero nuclei are determined in terms of the calculated 2BCDD's of the ground state and momentum-transfer *(q)* using the Plane Wave Born Approximation (PWBA), where the charge form factor is a Fourier transform of the ground state 2BCDD's and vice versa .

The calculated elastic longitudinal charge form factors *F(q)* for various closed and open 1s, 1p and 2s-1d shell nuclei with Z=N are carried out on the basis of equations of Ref [15] and equation (5). We have examined two cases for the form factors *F(q)* as those of the 2BCDD's, named case 1 and case 2 of Ref [15].

In figures (1) to (6), the calculated *F(q)*'s are compared with those of experimental data for ^{4}He, ^{12}C, ^{16}O, ^{28}Si, ^{32}S, and ^{40}Ca nuclei, respectively. Parts a and b of these figures are the calculated results based on case 1 and case 2 . In the above figures the calculated *F(q)*'s are plotted as a function of q while those of experimental data are plotted as a function of q_{eff}, where $q_{eff}=q\left[1+\frac{3}{2}\frac{ze^2}{E_i R_c}\right]$ and $R_c=\sqrt{\frac{5}{3}}\langle r^2\rangle^{1/2}$ [16],where E_i is initial energy and $\langle r^2\rangle^{1/2}$ is root mean square. The dashed and solid curves are the calculated *F(q)*'s without ($r_c=0$) and with ($r_c=0.5$fm) the inclusion of the effect of two-body short range correlation functions (SRC's), respectively whereas the dotted symbols are those of experimental data.

1. ^{4}He nucleus: The elastic longitudinal *F(q)*'s of ^{4}He nucleus is displayed in figure (1). As it is obvious from parts (a) and (b) of this figure that the solid curves are better in describing the experimental data [17,18] than those of the dashed curves. Since the solid curves in (a) and (b) agree quite well with the data up to q=3.2 fm^{-1} and underestimate these data at q > 3.2 fm^{-1}. Besides, these solid curves indicate that the inclusion of two-body SRC's tends to move the locations of the diffraction minima into the regions having less momentum transfer than those of dashed curves.

The quality of agreement between the calculated *F(q)*'s and those of experimental data even becomes better in part (b) than part (a) since the solid curve in (b) becomes closer to the data at higher momentum transfer of q > 3.2 fm^{-1} than that of part (a). Besides in part (b), the location of the diffraction minimum is reproduced in the correct place while in part (a) there is a shift of about Δq =0.15 fm^{-1} between the locations of the calculated and experimental diffraction minima as seen in the solid curves of this figure. It is concluded from this figure that considering the higher state $1p_{3/2}$ with occupation probability $\eta_{1p_{3/2}}$=0.2 together with the introduction of the two-body SRC's in the calculation (the solid curve of part b) leads to reproduce better result for the calculated *F(q)*'s than that of part a (case1).

2. ^{12}C nucleus: The elastic longitudinal form factors of ^{12}C nucleus are presented in figure (2). It is noticed from this figure that both the magnitude and the behavior of the calculated form factors in case 1 and case 2 are in a very good agreement with those of experimental data [19] throughout the whole range of momentum transfer q. Besides, the locations of the calculated diffraction minima in both cases are reproduced in the correct place. It is also noticed that the introduction of the two – body SRC's in the calculations of both cases (the solid curves) leads to enhance slightly the values of the calculated form factors in the region of momentum transfer $q \geq 1.7$ fm^{-1} and consequently tends to improve the calculated results of the form factors as seen by the solid curves since they

become closer to the experimental data than those of dashed curves. Inspection of parts (a) and (b) of this figure gives an indication that case 1 is better representing the experimental data of form factors in ^{12}C nucleus than that of case 2 .

***3. ^{16}O nucleus*:** In figure (3) we explore the calculated results for the form factors of ^{16}O nucleus. It is evident from this figure that the calculated results obtained in both cases are nearly the same. This is attributed to the chosen values of occupation probabilities in case 2 which are nearly the same as those of case 1. It seems that the calculated results of case 2 are not affected by the small change that we have done in the values of the occupation probabilities of case 2. However, the dashed and solid curves of both cases are in reasonable agreement with those of experimental data [19] up to momentum transfer q=2.8 fm^{-1}. The first diffraction minimum which is known from the experimental data is very well reproduced by the calculations of case 1 and case 2. It is seen from this figure that there is a disagreement between the experimental and calculated form factors of this nucleus at momentum transfer $q\approx 3$ fm^{-1} where it seems that there is a second diffraction minimum in the experimental data which cannot be reproduced in the correct place for both cases. This figure also demonstrates that the effect of the two–body SRC's starts at the region of momentum transfer $q \geq 3.1\,\text{fm}^{-1}$ where the solid curve, in both cases, deviates from the dashed curve at this region of q.

***4. ^{28}Si nucleus*:**The form factors of ^{28}Si are displayed in figure (4). It shows that the calculations of case 2 are better in reproducing the experimental data than that of case 1. In both calculations of case 1 and case 2 , the experimental data [20] of ^{28}Si nucleus are very well reproduced up to q=2.3 fm^{-1}. In the region of q >2.3 fm^{-1} of case 1, both the behavior and the magnitude of the calculated form factors dispredict the data. It is obvious that the calculated second diffraction minimum (located at $q \approx 2.7$ fm^{-1}) is not in agreement with that of experimental data (located at $q \approx 2.35$ fm^{-1}). Besides, the third diffraction minimum which is presented in the experimental data (located at $q\approx 3.4$ fm^{-1}) is not reproduced by the calculation of case 1. It is seen that the effect of the two-body SRC's begins at the region of momentum transfer $q \geq 2.8$ fm^{-1} (see the solid curve in case 1) and leads to reduce the enhancement of the calculated result of the form factors. While in case 2, this effect starts at the region of q =1.25 fm^{-1} (see the solid curve in case 2) and leads to increase the enhancement of the calculated form factors which consequently tends to improve the calculated result of case 2. It is noted, in case 2, that the behavior of the calculated results (the solid curve) is in a very good agreement with that of the experimental data throughout the whole range of q. Besides, the first, second and third diffraction minima which are presented in the experimental data are quite well described by the solid curve. It is also noted that the solid curve of case 2 underestimates the data at the region of momentum transfer $q \geq 2.3$ fm^{-1}.

***5. ^{32}S nucleus*:** The form factors of ^{32}S nucleus are presented in figure (5). It is very clear that there is a disagreement between the calculated result of case 1 and those of experimental data [20]. Where the behavior, the magnitude of the calculated form factors at $q \geq 1.2$ fm^{-1} and the locations of the calculated diffraction minima are not in accordance with the experimental data in this case. While in case 2, the calculated result of the form factors are in good agreement with those of experimental data up to the region of momentum transfer $q \approx 3$fm^{-1}. The behavior of the calculated results are also in very well accordance with the data. In addition, all the experimental diffraction minima of this nucleus are reproduced in the correct places as seen in the solid curve of case 2. This figure shows that the effect of the two – body SRC's is small up to $q \approx 2.7$ fm^{-1} while for higher q it becomes progressively larger since it reduces the calculated form factor significantly at this region of q as seen in the solid curves of case 1 and case 2 .

***6. ^{40}Ca nucleus*:** Figure (6) demonstrates the form factors of ^{40}Ca nucleus. It is noted from case 1 that the calculated form factors are in a good agreement with those of experimental data [21] for all range of q with the exception of the region 1 fm^{-1} < q < 2 fm^{-1}. In this region, the calculated form factors underestimate slightly the experimental data and the calculated second diffraction minimum is not reproduced in the correct place. In fact, an improvement for the calculated form factors is obtained with considering the higher state $2p_{3/2}$ in the calculations of case 2. Since the occupation

probability of this state is taken as $\eta_{2p_{3/2}}$=0.15 . As it is evident from case 2 of this figure that there is a very good agreement between the calculated and experimental form factors throughout the whole range of momentum transfer *q*. Here, both of the behavior and magnitude of the calculated curves are in a very good agreement with those of experimental data. Besides, the calculated first and second diffraction minima are in coincidence with those of the experimental data. The same argument can be applied here for the effect of the two-body SRC's as that of figure (5), i.e. the effect is small up to $q \approx 2.8$ fm^{-1} whereas for higher *q* it becomes larger and it decreases the calculated form factors as seen in the solid curves of case 1 and case 2.

Finally the effect of higher occupation probabilities and SRC's are well established for the analysis of elastic scattering and we see good agreement between the calculated elastic longitudinal *F(q)*'s and those of experimental data.

REFERENCES:

[1]J.Dubach, J.H. Koch and T.W. Donnelly; Nucl. Phys., **A271**, 279, (1976).
[2]T. Sato,N.Odagawa,H.Ohtsubo and T.S. Lee; Phys .Rev.,**C49**,776,(1994).
[3]J. Bergstrom,S. Kowalski and R.Neuhausen ; Phys.Rev.,**C25**,1156, (1982).
[4] J.D. Walecka; Nucl. Phys., **A574**, 271, (1963).
[5]C.Ciofi Degli Atti; Phys. Rev., **175**,1256 , (1968).
[6]F.C.Khanna; Phys. Rev. Lett., **20**,871, (1968).
[7]C.Ciofi Degli Atti and N.M.Kabachnik; Phys. Rev., **C1**,809, (1970).
[8]J.C.Bergstrom,W.Bertozzi,S. Kowalski,X. K.Maruyama, J.W.Lightbody, S.P.Fivozinsky and S.Penner; Phys. Rev. Lett., **24**,152,(1970).
[9]W.Reuter,G.Fricke,K.Merle and H.Miska; Phys. Rev., **C26**, 806,(1982).
[10] S.E.Massen and C.Moustakidis ; Phys. Rev., **C60**, 024005, (1999).
[11]C.Moustakidis and S.E.Massen ; Phys. Rev., **C62**, 034318, (2000).
[12]R.A.Radhi ; Eur. Phys. J., **A16**, 387, (2003).
[13]T. de Forest and J.D.Walecka ; Adv.Phys., **15**,1,(1966).
[14]H.Uberall, "Electron Scattering From Complex Nuclei. Part B", Academic Press, New York, (1971).
[15]F.I. Shrrad; Ph.D.thesis, College of Science, University of Baghdad, (2007).
[16]B.A.Brown,R.A.Radhi and B.H.Wildenthal; Phys. Rep., **101**,313 (1983).
[17]J.S.McCarthy,I.Sick and R.R.Whitney; Phys. Rev .,**C15**, 1396, (1977).
[18]R.F.Frosch, J.S.McCarthy, R.E.Rand and M.R.Yearian ; Phys. Rev., **160**, 874,(1967).
[19]I. Sick and J.S.McCarthy ; Nucl. Phys., **A150**, 631 ,(1970).
[20]G.C.Li ,M.R.Yearian and I. Sick; Phys. Rev., **C9**, 1861, (1974).
[21]B.B.Sinha,G.A.Peterson,R.R.Whitney,I.Sick and J.S.McCarthy; Phys. Rev., **C7**, 1930, 1973).

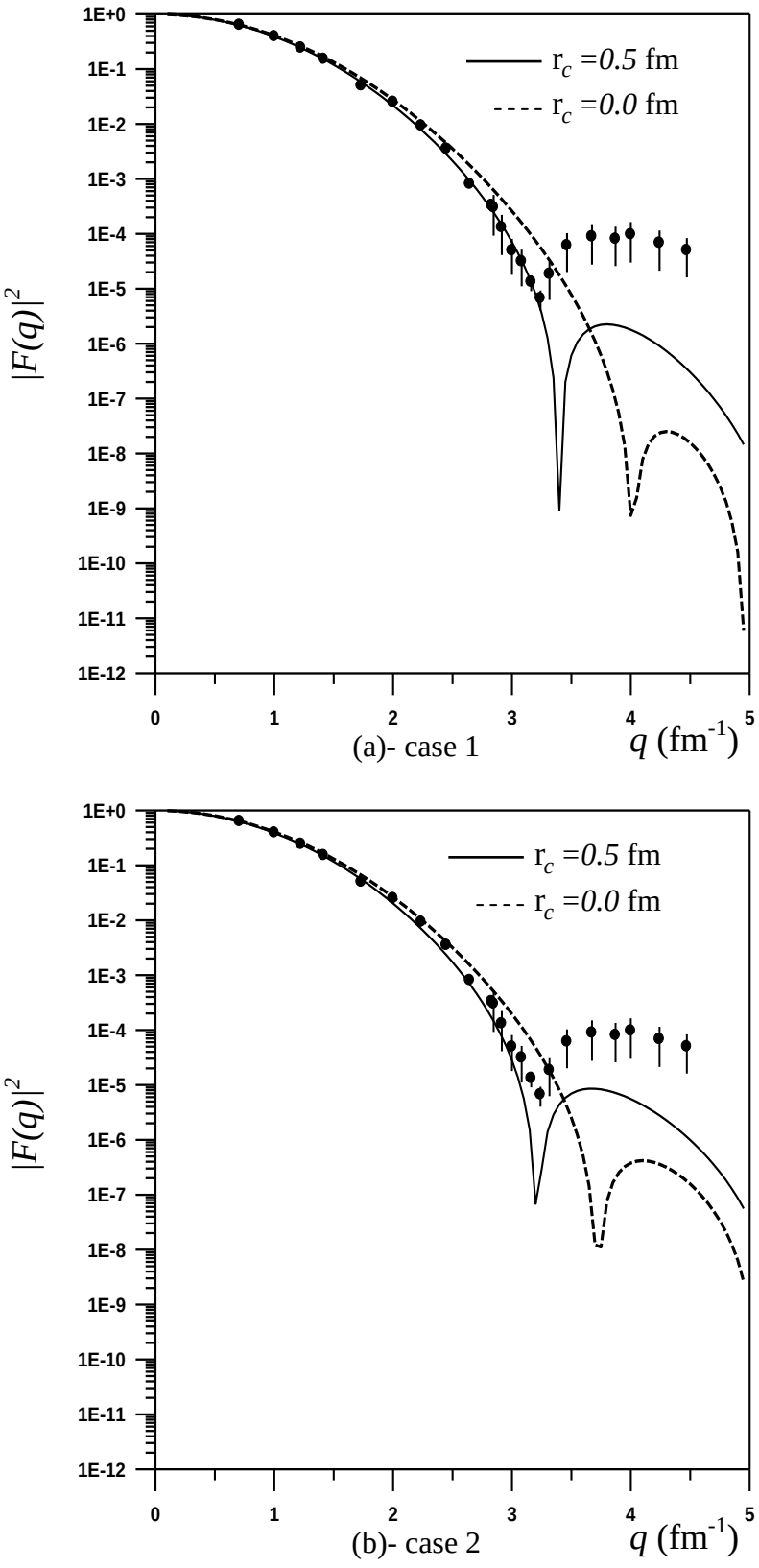

Figure (1): Elastic form factors for ^4He nucleus. The dotted symbols are the experimental data of Ref [17,18].

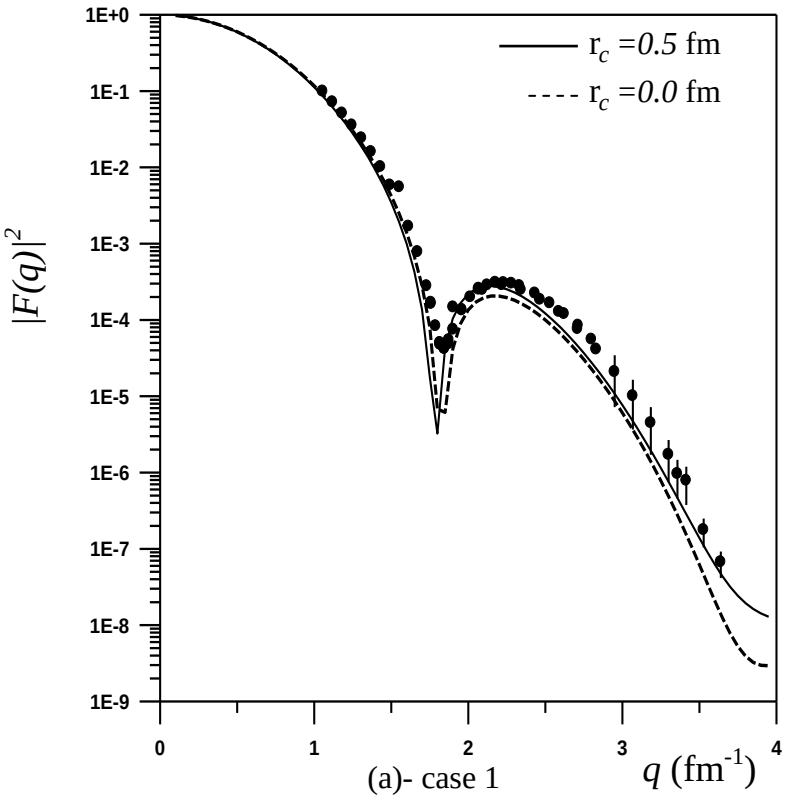

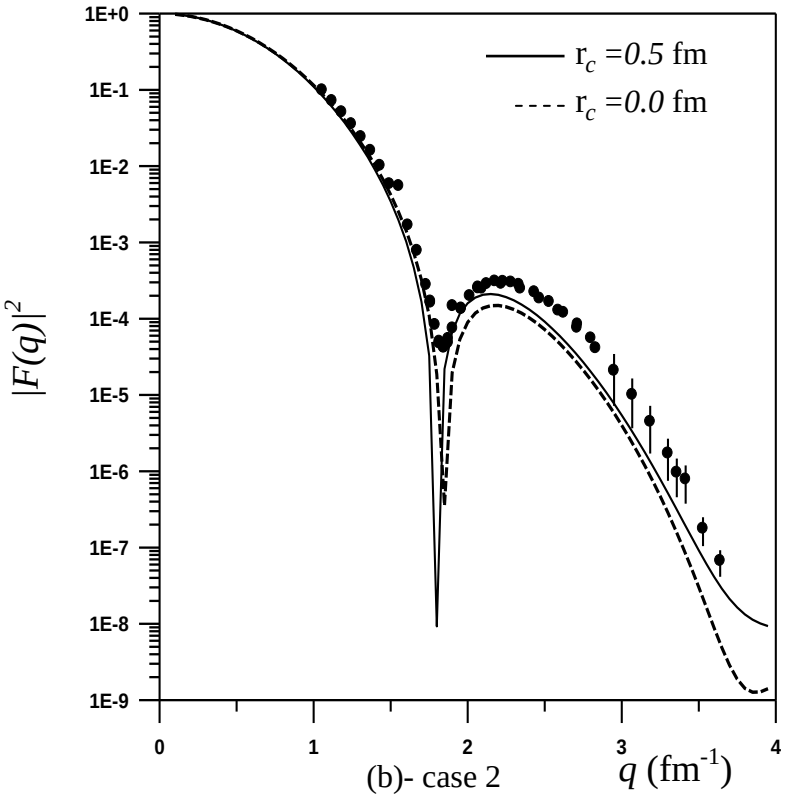

Figure (2): Elastic form factors for ^{12}C nucleus. The dotted symbols are the experimental data of Ref [19].

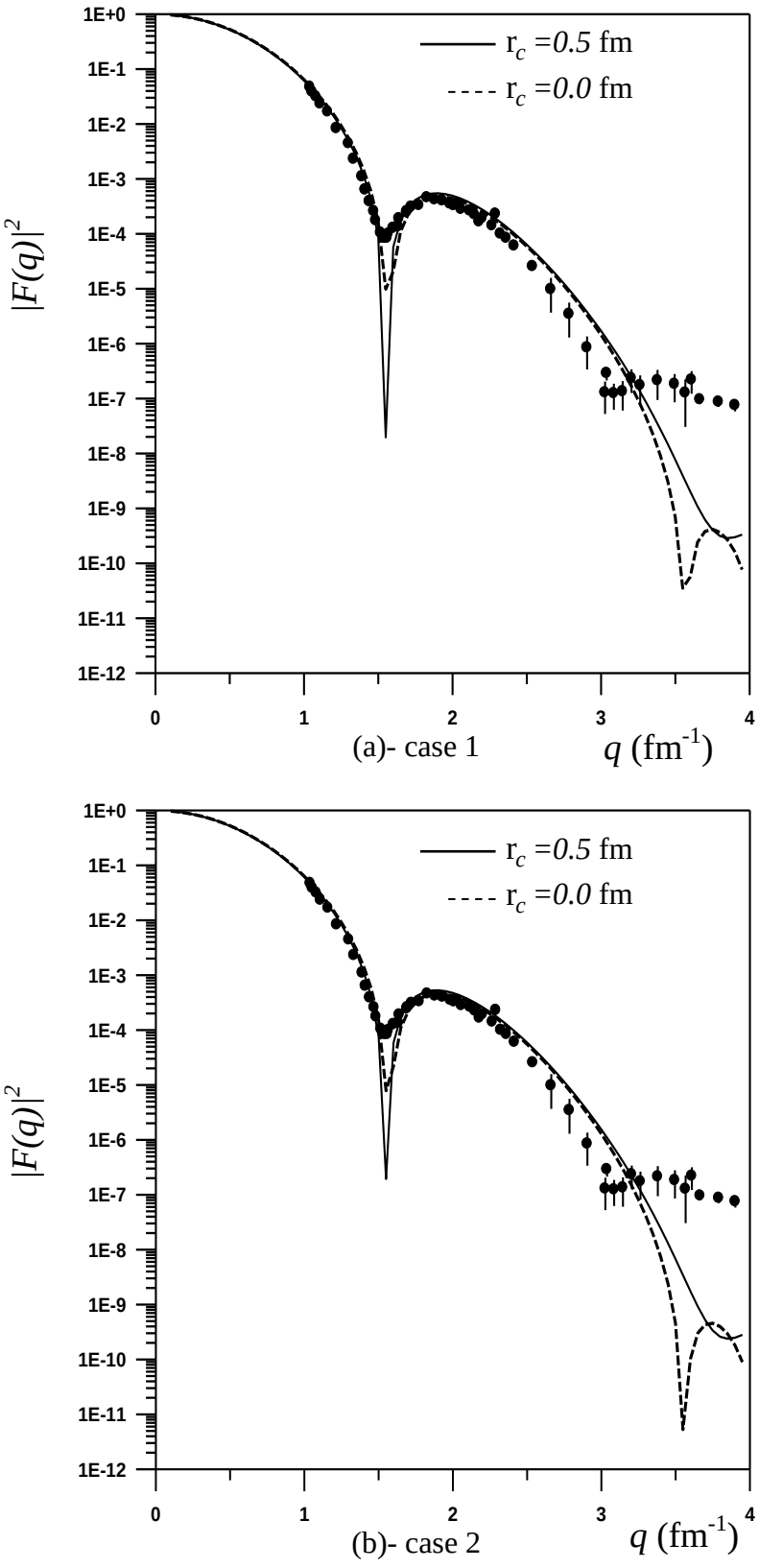

Figure (3): Elastic form factors for ^{16}O nucleus. The dotted symbols are the experimental data of Ref [19].

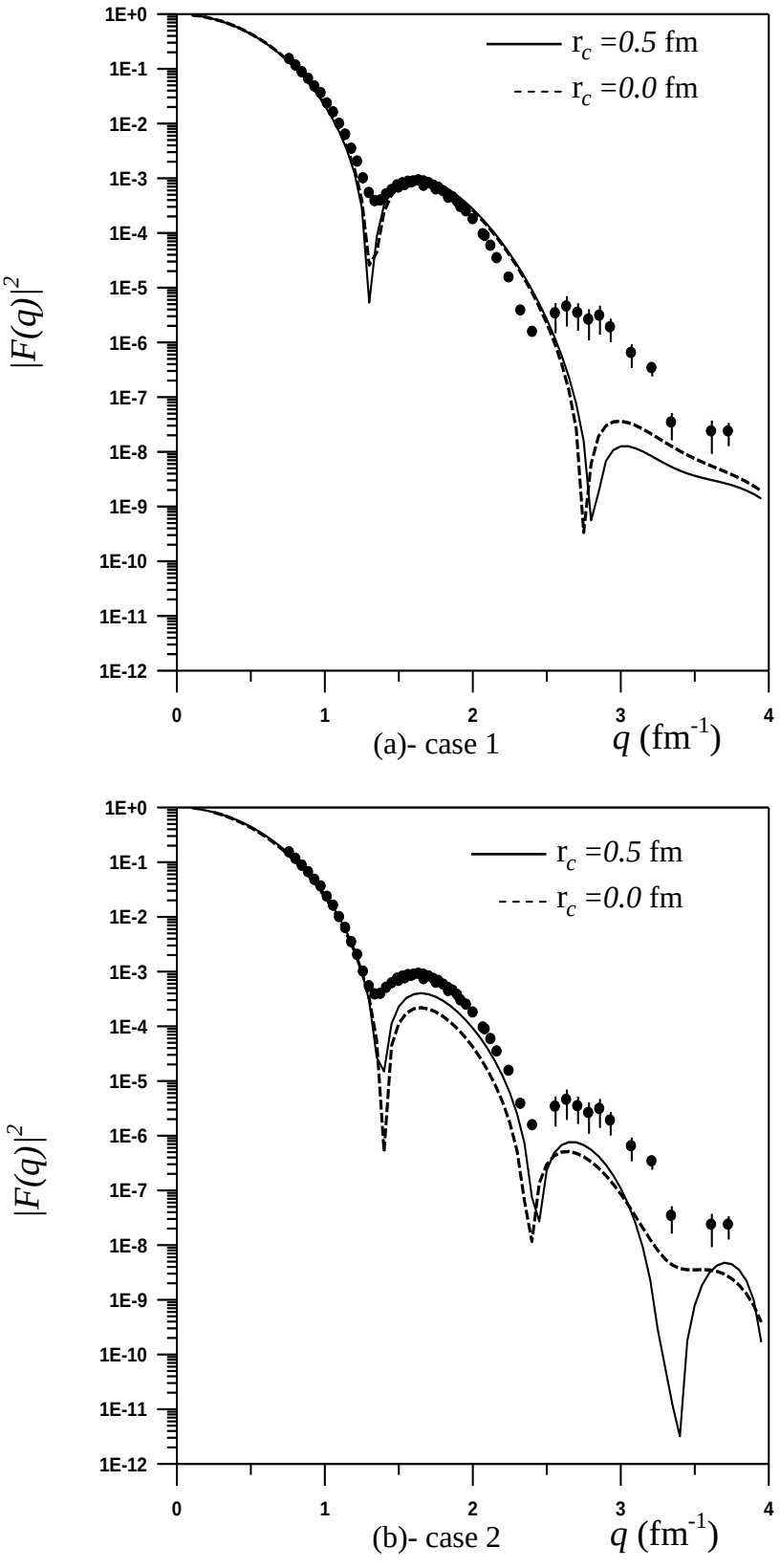

Figure (4): Elastic form factors for ^{28}Si nucleus. The dotted symbols are the experimental data of Ref [20].

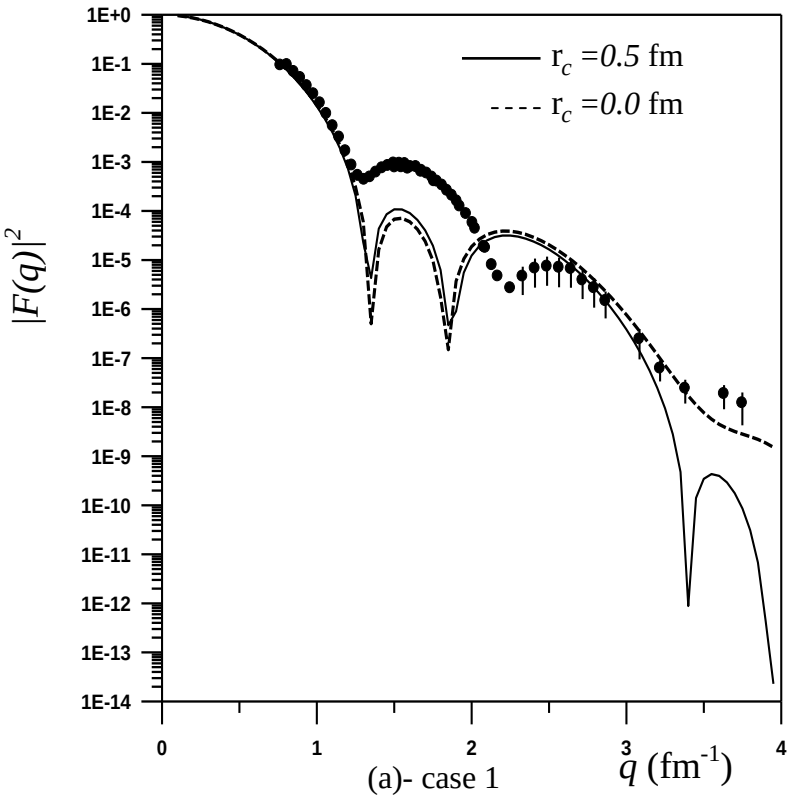

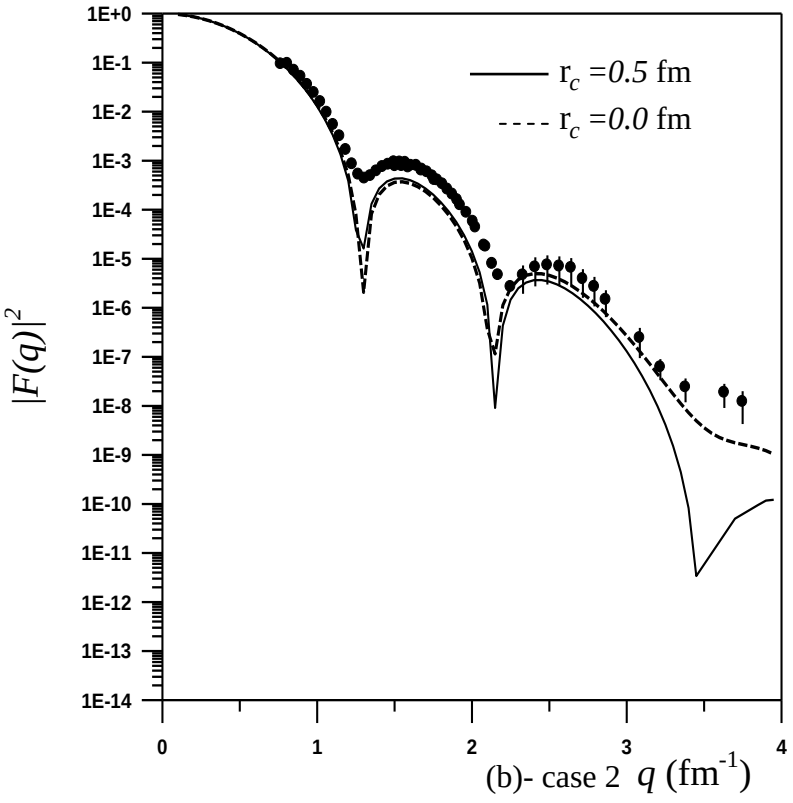

Figure (5): Elastic form factors for ^{32}S nucleus. The dotted symbols are the experimental data of Ref [20].

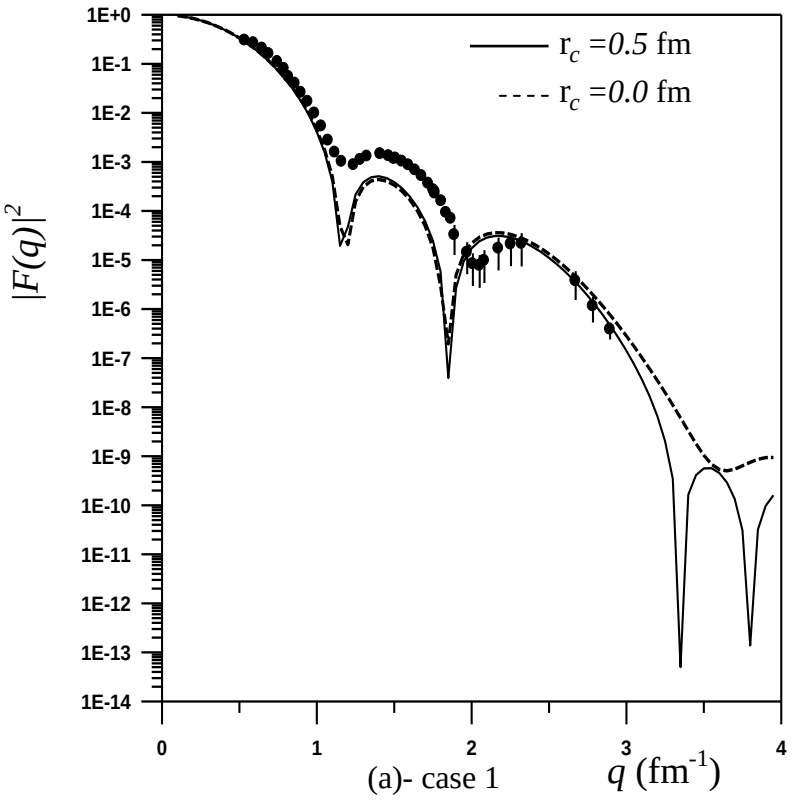

(a)- case 1

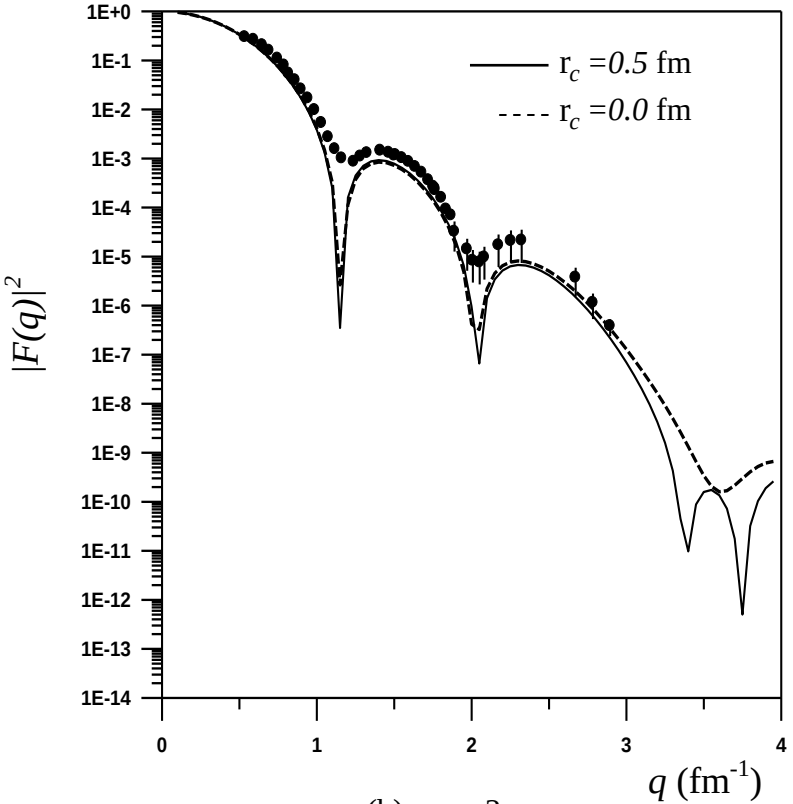

(b)- case 2

Figure (6): Elastic form factors for ^{40}Ca nucleus. The dotted symbols are the experimental data of Ref [21].